

This article was downloaded by:

On: 25 January 2011

Access details: *Access Details: Free Access*

Publisher *Taylor & Francis*

Informa Ltd Registered in England and Wales Registered Number: 1072954 Registered office: Mortimer House, 37-41 Mortimer Street, London W1T 3JH, UK



## Liquid Crystals

Publication details, including instructions for authors and subscription information:

<http://www.informaworld.com/smpp/title~content=t713926090>

### Organic electroluminescence using polymer networks from smectic liquid crystals

Matthew P. Aldred<sup>a</sup>; Miguel Carrasco-Orozco<sup>b</sup>; Adam E. A. Contoret<sup>b</sup>; Dewen Dong<sup>c</sup>; Simon R. Farrar<sup>b</sup>; Stephen M. Kelly<sup>a</sup>; Stuart P. Kitney<sup>a</sup>; Dean Mathieson<sup>b</sup>; Mary O'Neill<sup>b</sup>; W. Chung Tsoi<sup>b</sup>; Panos Vlachos<sup>a</sup>

<sup>a</sup> Department of Chemistry, University of Hull, Hull, HU6 7RX, UK <sup>b</sup> Department of Physics, University of Hull, Hull, HU6 7RX, UK <sup>c</sup> Department of Chemistry, Northeast Normal University, Changchun, Jilin Province, PRC

**To cite this Article** Aldred, Matthew P. , Carrasco-Orozco, Miguel , Contoret, Adam E. A. , Dong, Dewen , Farrar, Simon R. , Kelly, Stephen M. , Kitney, Stuart P. , Mathieson, Dean , O'Neill, Mary , Tsoi, W. Chung and Vlachos, Panos(2006) 'Organic electroluminescence using polymer networks from smectic liquid crystals', *Liquid Crystals*, 33: 4, 459 – 467

**To link to this Article:** DOI: 10.1080/02678290500487073

**URL:** <http://dx.doi.org/10.1080/02678290500487073>

PLEASE SCROLL DOWN FOR ARTICLE

Full terms and conditions of use: <http://www.informaworld.com/terms-and-conditions-of-access.pdf>

This article may be used for research, teaching and private study purposes. Any substantial or systematic reproduction, re-distribution, re-selling, loan or sub-licensing, systematic supply or distribution in any form to anyone is expressly forbidden.

The publisher does not give any warranty express or implied or make any representation that the contents will be complete or accurate or up to date. The accuracy of any instructions, formulae and drug doses should be independently verified with primary sources. The publisher shall not be liable for any loss, actions, claims, proceedings, demand or costs or damages whatsoever or howsoever caused arising directly or indirectly in connection with or arising out of the use of this material.

# Organic electroluminescence using polymer networks from smectic liquid crystals

MATTHEW P. ALDRED<sup>†</sup>, MIGUEL CARRASCO-OROZCO<sup>‡</sup>, ADAM E.A. CONTORET<sup>‡</sup>, DEWEN DONG<sup>§</sup>, SIMON R. FARRAR<sup>‡</sup>, STEPHEN M. KELLY<sup>\*†</sup>, STUART P. KITNEY<sup>†</sup>, DEAN MATHIESON<sup>‡</sup>, MARY O'NEILL<sup>\*‡</sup>, W. CHUNG TSOI<sup>‡</sup> and PANOS VLACHOS<sup>†</sup>

<sup>†</sup>Department of Chemistry, University of Hull, Cottingham Rd., Hull, HU6 7RX, UK

<sup>‡</sup>Department of Physics, University of Hull, Cottingham Rd., Hull, HU6 7RX, UK

<sup>§</sup>Department of Chemistry, Northeast Normal University, Changchun Jilin Province, PRC

(Received 15 August 2005; accepted 2 October 2005)

We report the synthesis of a red light-emitting and photopolymerizable smectic liquid crystal (reactive mesogen). We investigate the suitability of polymer networks formed from smectic reactive mesogens for use in organic light-emitting diodes (OLEDs). The use of mixtures of smectic reactive mesogens is shown to lower the processing temperature for the fabrication of OLEDs to room temperature. We also report efficient energy transfer from a nematic polymer network host to a smectic light-emitting dopant and polarized emission from a polymer network formed from an aligned smectic reactive mesogen.

## 1. Introduction

One of the research challenges for organic light-emitting diodes (OLEDs) is the development of a solution-processable, red-green-blue pixellated display. The use of insoluble films of light-emitting and/or charge-transporting polymer networks appears a very attractive approach to fabricating such displays [1–9]. For example, a full-colour OLED was demonstrated using polymer network pixels formed by photopolymerizing mainchain polyfluorenes with photo-crosslinkable oxetane sidechains and a photoacid as a cationic initiator [1]. Another, perhaps more attractive, approach uses liquid crystalline polymer networks formed from polymerizable light-emitting liquid crystals (reactive mesogens, RMs) [2–9]. Light-emitting and charge-transporting RMs can be photolithographically patterned, often without a photoinitiator, to fabricate solution-processable, multilayer OLEDs with small, well resolved pixels [2–9]. However, all of the OLEDs reported so far using this approach have used light-emitting and/or charge-transporting polymer networks formed by polymerising *nematic* monomers [2–15]. We wished to determine whether the increased order of *smectic* liquid crystals might be of potential benefit for OLEDs with improved performance. The layered structure of smectic liquid crystals is known to lead to

high charge carrier mobility [16–20], which should in turn, at least in theory, lead to more efficient OLEDs.

To date, a small number of smectic RMs have been prepared for use as charge carrying organic semiconductors with applications in organic field effect transistors (OFETs) [21–25]. The short and long range order present in the layered structure of highly ordered smectic phases, or ‘plastic crystals’, leads to a high charge carrier mobility, but these are difficult to process and align in an OLED configuration. However, the magnitude of the carrier mobility of the least ordered smectic phases (smectic A and smectic C) may well be sufficient for OLEDs. Therefore, we now report the performance of light-emitting and *smectic* RMs designed specifically for use as the emissive layer in OLEDs. These RMs exhibit either a SmA or SmC phase with red, green or blue emission and a satisfactory charge carrier mobility for use in OLEDs. Most smectic RMs reported to date exhibit high melting points. Therefore, we have prepared light-emitting smectic RM mixtures with low melting points in order to facilitate room temperature device processing.

## 2. Results and discussion

### 2.1. Synthesis

The synthetic details of the preparation of most of the materials mentioned in this report are described elsewhere [25]. The synthesis of the red chromophore 9

\*Corresponding authors. Email: S.M.Kelly@hull.ac.uk and M.Oneill@hull.ac.uk

involved the bromination of commercially available 2,1,3-benzothiadiazole in the 4,7-position according to the literature, see scheme 1 [26]. A Stille coupling [27] of commercially available 2-(tributylstannyl)thiophene and compound **1** using Pd(PPh<sub>3</sub>)<sub>4</sub> as the catalyst, afforded the symmetrical bis-thiophene compound **2**. During the work-up procedure the reaction mixture was washed with a potassium fluoride solution to remove the tin side products. Lithiation of the protected THP phenol **5**, *n*-BuLi followed by reaction with 2-isopropoxy-4,4,5,5-tetramethyl-1,3,2-dioxaborolane, gave the boronic ester derivative **6** [28]. Subsequent treatment of compound **2** with *N*-bromosuccinimide (purified by recrystallization from water) resulted in the brominated analogue **3**, which was coupled to compound **6** in an anhydrous Suzuki cross-coupling reaction [29] to afford the protected symmetrical compound **7**. Deprotection with *p*-toluene sulphonic acid monohydrate afforded the bis-phenol **8**, which was alkylated using a bromodiene ester [12] in a Williamson ether synthesis [30] to yield the red chromophore **9**.

## 2.2. Mesomorphic properties

The mesomorphic behaviour of compound **9** was investigated between cross polarizers using optical microscopy. An enantiotropic smectic C phase (SmC) was the only one observed. A schlieren texture with 4-brush disclinations can be seen in the liquid crystal phase and droplets are not seen on cooling slowly from the isotropic phase on forming the smectic C phase. The liquid crystalline properties of **9** were also confirmed by DSC. Figure 1 shows the differential scanning calorimetry (DSC) measurement. A melting peak transition is observed at 146°C in both the first and second heating cycles, with subsequent crystallization peaks on the cooling cycles. A clearing point transition with a comparatively weak enthalpy change is also observed at 185°C.

## 2.3. OLED fabrication and physical measurements

The pyridine **10**, pyrimidine **11** and tetrazine **12** collated in table 1 differ only in the number of nitrogen atoms and C–H units in the central heterocyclic ring A, see table 1. Compounds **10** and **11** exhibit a smectic C phase, whereas compound **12** is not liquid crystalline.

Molecular modelling shows that compounds **10** and **11** exhibit significant inter-annular twisting (40°) around the bond between one of the phenyl rings and the heterocyclic ring, see figure 2, due to electrostatic repulsion between the hydrogen atoms in an *ortho* position to the inter-annular bond. This limits the overlap of the  $\pi$ -electrons in the 2p<sub>z</sub> orbitals on the

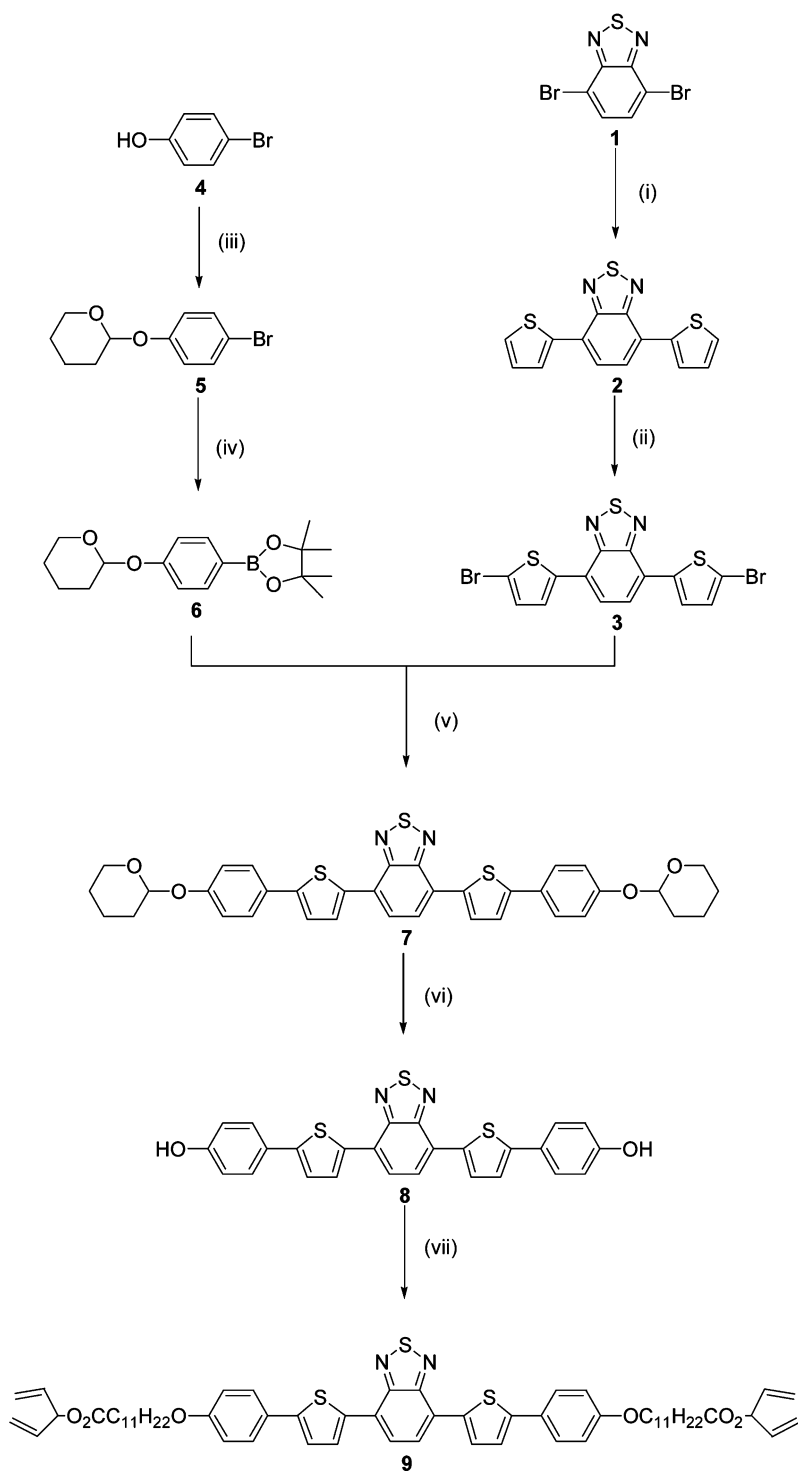
aromatic rings. This contributes to the blue emission ( $\lambda_{\text{max}} \approx 440$  nm) shown in the PL spectra of compound **10**, see figure 3. There is almost no inter-annular twisting (0–1°) in compound **12** due to the electrostatic attraction between the hydrogen atom and the adjacent lone pair electrons on the nitrogen atoms of the adjacent tetrazine ring. Therefore, the aromatic core is essentially planar with a high degree of  $\pi$ -electron overlap and charge delocalization. This leads to a very significant red shift (100 nm) and orange–red fluorescence ( $\lambda_{\text{max}} \approx 540$  nm).

The ionization potential and electron affinity exhibit the lowest values for the pyridine **10** (5.40 and 2.07 eV, respectively) intermediate values for the pyrimidine **11** (5.57 and 2.1 eV) and the highest values for the tetrazine **12** (5.67 and 3.58 eV). These trends are a reflection of the presence of an increasing number of electron-deficient nitrogen atoms in the aromatic molecular core and the differences in the band gap; by comparison, the corresponding terphenyl derivative, with no nitrogen atoms, exhibits an even lower ionization potential and electron affinity (5.31 and 1.75 eV).

The low melting point of the benzothiadiazole compounds **13–15**, shown in table 2, enables ternary mixtures (1:1:1) to be prepared with a melting point below room temperature and enantiotropic smectic C and A phases above it (Cr–SmC = <–50°C; SmC–SmA = 60°C; SmA–I = 72°C) according to DSC measurements. However, as commonly occurs in this kind of organic material, the mixture is meta-stable and crystallizes over time [23]. However it is stable long enough at room temperature for its physical properties to be investigated and for the photolithographic cross-linking of devices. Hence we show that preparing mixtures of compounds with the same aromatic cores allows room temperature, rather than high temperature, photolithographic processing and pixelization without modifying the band-energies of the materials.

The ionization potential and electron affinity are lower for the thiadiazole **13** (5.34 and 2.68 eV) than those of the oxadiazole **16** (5.42 and 2.87 eV). This is a reflection of the presence of the electron-deficient oxygen atom in **16** in place of the electron-rich sulphur atom in the aromatic molecular core of **13**. Therefore, the thiadiazoles (**13–15**) exhibit green light, see figure 3 for the PL spectrum of compound **14**. The oxadiazole **16**, with an oxygen atom in place of the sulphur atom, emits orange light ( $\lambda_{\text{max}} \approx 540$  nm), i.e. the emission is red-shifted (40 nm) compared with that ( $\lambda_{\text{max}} \approx 500$  nm) of the corresponding thiadiazole **14**.

The charge carrier mobility of the 1:1:1 ternary mixture of **13–15** was determined by a standard photocurrent time-of-flight method. Similar transients



Scheme 1. Reagents and conditions: (i)  $\text{Pd}(\text{PPh}_3)_4$ , DMF,  $90^\circ\text{C}$ , (ii) NBS,  $\text{CH}_3\text{CO}_2\text{H}$ ,  $\text{CHCl}_3$ ,  $65^\circ\text{C}$ , (iii) 3,4-dihydro-2H-pyran, PTSA, room temperature, (iv) (a) *n*-BuLi, THF,  $-78^\circ\text{C}$ , (b) 2-isopropoxy-4,4,5,5-tetramethyl-1,3,2-dioxaborolane, (v)  $\text{Pd}(\text{PPh}_3)_4$ ,  $\text{K}_3\text{PO}_4$ , DMF,  $90^\circ\text{C}$ , (vi) PTSA,  $\text{CH}_2\text{Cl}_2$ : $\text{C}_2\text{H}_5\text{OH}$  (1:1), room temperature, (vii) 1,4-pentadien-3-yl 12-bromododecanoate,  $\text{K}_2\text{CO}_3$ , DMF,  $90^\circ\text{C}$ .

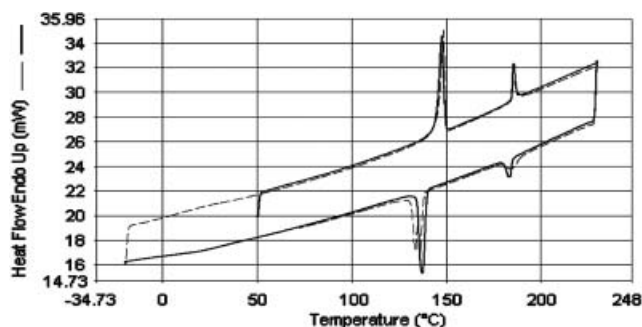
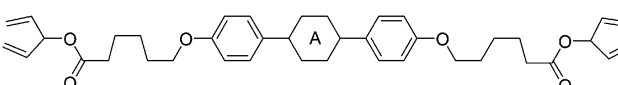
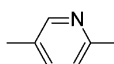
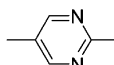
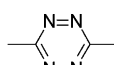


Figure 1. DSC scan for the red chromophore **9**, first (full line) and second (dashed line) heating and cooling cycles,  $10^{\circ}\text{C min}^{-1}$ .

are obtained for both electrons and holes. Two distinct mechanisms for carrier transport are suggested and will be discussed in more detail elsewhere. The hopping of carriers between the aromatic cores of the smectic liquid crystal gives a room temperature mobility of  $1 \times 10^{-3} \text{ cm}^2 \text{ V}^{-1} \text{ s}^{-1}$  for both electron and holes. This compares well with hole mobility values of  $2 \times 10^{-5} \text{ cm}^2 \text{ V}^{-1} \text{ s}^{-1}$  obtained from nematic crosslinked RMs [31]. However, many carriers are trapped and the emptying of shallow traps gives a long-lived tail in the time-of-flight transients. A multilayer liquid crystalline polymer network OLED incorporating compound **14** was fabricated as described above. Green emission was observed ( $\lambda_{\text{max}} \approx 500 \text{ nm}$ ) with a maximum efficiency of

Table 1. Liquid crystalline transition temperatures ( $^{\circ}\text{C}$ ) of the heterocycles **10–12**.



Compound	Ring A	Cr	SmC	I	
<b>10</b>		•	87	•	•
<b>11</b>		•	25	•	•
<b>12</b>		•	109	–	•

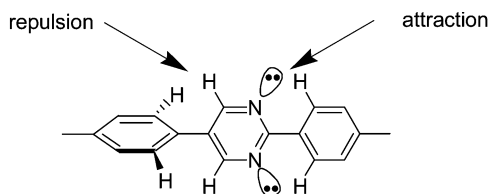


Figure 2. Inter-annular twisting between a phenyl ring and a pyrimidine ring.

$0.05 \text{ cd A}^{-1}$  at  $50 \text{ cd m}^{-2}$  at 6 V, and a maximum brightness of  $160 \text{ cd m}^{-2}$  at 12 V as shown in figure 4. This is the first OLED using a smectic liquid crystalline polymer network. TAZ has a high barrier for electron injection so that improved performance would be expected from a hole blocking top layer with a larger electron affinity.

Polarized PL emission was obtained from the photochemically crosslinked polymer network of compound **14** uniformly oriented on a rubbed PEDOT surface, see figure 5. A maximum polarization ratio ( $=\text{PL}_{\parallel}/\text{PL}_{\perp}$ ) of 5:1 is obtained at 525 nm. This is a low value compared with those obtained using liquid crystalline mainchain polymers [32–35] and rigid rod oligomers [36, 37] or the corresponding nematic RMs [2–10]. The low ratio may be due to competition between the elastic forces from the alignment surface and those maintaining the smectic layer structure. However, increasing the length of the aromatic core of the smectic RM should give a higher order parameter and higher polarization ratio. Unfortunately, this would also probably give rise to a high melting point and a low degree of solubility in organic solvents at room temperature. For example, the red chromophore **9**

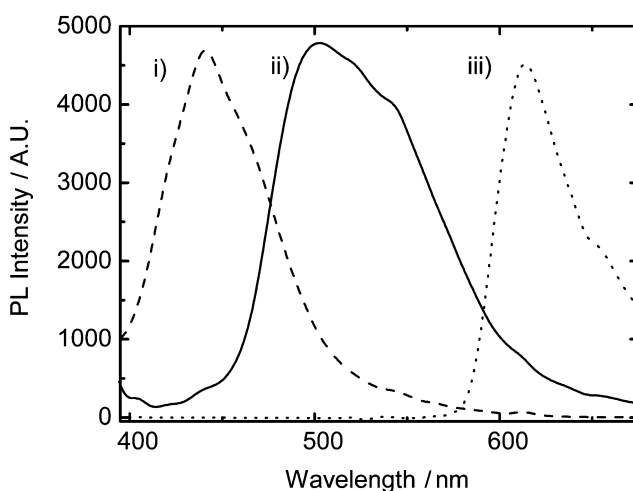
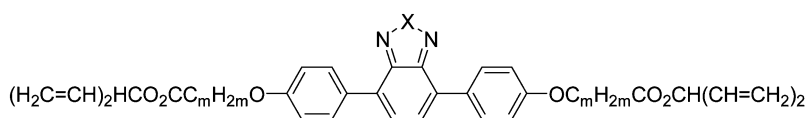


Figure 3. Solid state PL spectra of non-polymerized monomers (i) **10** (blue), (ii) **14** (green) and (iii) **12** (red).

Table 2. Liquid crystalline transition temperatures ( $^{\circ}\text{C}$ ) of the heterocycles **13**–**16**.

Compound	X	m	Cr	SmA	I
<b>13</b>	S	5	•	69	84
<b>14</b>	S	7	•	57	73
<b>15</b>	S	10	•	64	77
<b>16</b>	O	5	•	60	98

exhibits a smectic C phase at much higher temperatures (Cr–SmC=146 $^{\circ}\text{C}$ ; SmC–I=185 $^{\circ}\text{C}$ ) than those of compounds shown in table 2, due to the presence of two additional 2,5-disubstituted thiophene rings, i.e. a greater length-to-breadth ratio. The preparation of similar materials with lateral substituents, such as 9,9-dialkylfluorene derivatives [2–10, 32–35], which is the usual approach used to address these problems, also gives rise to a nematic phase as a consequence of the steric interactions used to increase the intermolecular distance. For example, the use of very short alkyl chains in 9,9-dialkylfluorene oligomers does lead to the formation of smectic phases, but the oligomers exhibit high melting points [38]. The electron-rich thiophene rings present in compound **9** also induce a substantial red-shift in the PL emission ( $\lambda_{\text{max}} \approx 650 \text{ nm}$ ) as expected.

The melting point of compound **9** is too high for room temperature processing so it has been used as a red dopant in a green emitting nematic polymer network host compound **17**, see figure 6.

Figure 7 shows the PL spectrum of a guest–host mixture containing 1 wt% of **9**. The emission spectrum

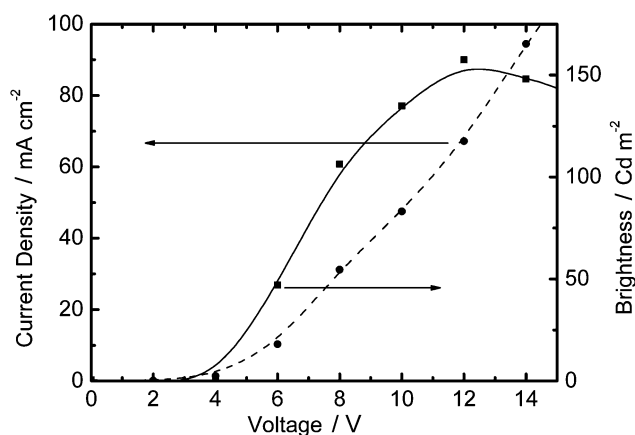


Figure 4. Current and luminance versus voltage characteristics of an OLED containing **14** as a polymer network.

from the undoped host is also shown. In the doped system, non-radiative Förster energy transfer results in red emission with only residual PL from the host [39]. An OLED was fabricated incorporating **9**; 75  $\text{cd m}^{-2}$  was obtained at a voltage of 20 V with an efficiency of 0.2  $\text{cd A}^{-1}$ .

The devices reported above present a real advance on other reports of electroluminescence from smectic liquid crystals, which are not RMs. Previously electroluminescence was reported from smectic cells, rather than solution processed thin films, with very thick emission layers (2–3  $\mu\text{m}$ ), which resulted in very high driving voltages (150–280 V) [40, 41]. One cell was heated to 70 $^{\circ}\text{C}$  to obtain electroluminescence in the high temperature smectic phase [40]. The other cell used a guest–host effect to align a light-emitting coumarin 6 laser dye in a non-emitting smectic host at 90 $^{\circ}\text{C}$  [41]. However the results discussed here for a smectic RM are not as good as for nematic RMs which show efficiencies up to

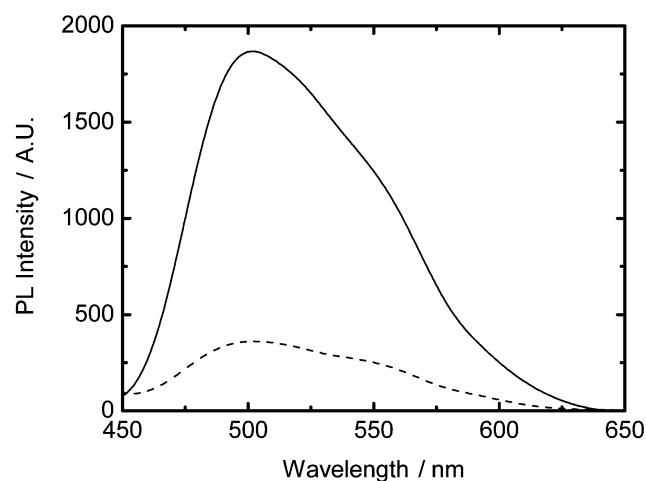


Figure 5. PL from compound **14** as a polymer network: parallel (full line) and perpendicular (dashed line) to the rubbing direction of the underlying rubbed PEDOT alignment layer.

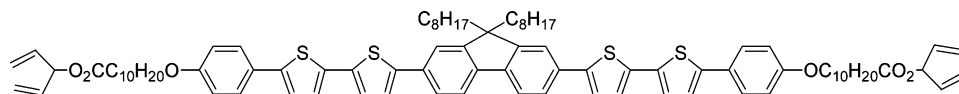


Figure 6. Chemical structure of the green RM host, i.e. compound **17** [8].

4.3 lm W<sup>-1</sup> and luminances up to 1000 cd m<sup>-2</sup> at 10 V [2, 8, 15, 42].

### 3. Experimental

#### 3.1. Synthesis

Scheme 1 illustrates the synthetic pathway used in the synthesis of compound **9**. All commercially available starting materials, reagents and solvents were used as supplied (unless otherwise stated) and were obtained from Aldrich, Strem Chem. Inc., Acros or Lancaster Synthesis. All reactions were carried out using a dry nitrogen atmosphere unless water was present as solvent or reagent, and the temperatures were measured internally. Mass spectra were recorded using a Gas Chromatography/Mass Spectrometer (GC/MS)-QP5050A Shimadzu with Electron Impact (EI) at a source temperature of 200°C. Compounds with an RMM >800 g mol<sup>-1</sup> were analysed using a Bruker, reflex IV, Matrix Assisted Laser Desorption/Ionisation (MALDI), Time of Flight (TOF) MS. A 384 well microlitre plate format was used with a scout target. Samples were dissolved in DCM with HABA (2-(4-hydroxyphenylazo)benzoic acid) matrix (1:10, respectively). The mass ion of the material is identified as M<sup>+</sup>. <sup>1</sup>H NMR spectra were recorded using a JEOL Lambda

400 spectrometer using an internal standard of tetramethylsilane (TMS). GC was carried out using a Chromopack CP3800 gas chromatograph equipped with a 10 m CP-SIL 5CB column. Purification of intermediates and final products was mainly accomplished by gravity column chromatography, using silica gel (40–63 μm, 60 A) obtained from Fluorochem. The melting point and liquid crystal transition temperatures of the solids prepared were measured using a Linkam 350 hot stage and control unit in conjunction with a Nikon E400 polarizing microscope. The transition temperatures of all of the final products were confirmed using a Perkin-Elmer DSC-7 in conjunction with a TAC 7/3 instrument controller, using the peak measurement for the reported value of the transition temperatures. The purity of the final compound (**9**) was checked by elemental analysis using a Fisons EA 1108 CHN analyser.

**3.1.1. 4,7-bis(Thien-2-yl)-2,1,3-benzothiadiazole (2).** A mixture of 4,7-dibromo-2,1,3-benzothiadiazole (**1**) (5.00 g, 0.0170 mol), 2-(tributylstannyl)thiophene (15.7 g, 0.0421 mol) and tetrakis(triphenylphosphine) palladium(0) (0.30 g, 2.6 × 10<sup>-4</sup> mol) in DMF (50 cm<sup>3</sup>) was heated at 80°C for 24 h. Dichloromethane (200 cm<sup>3</sup>) was added to the cooled reaction mixture. The resultant solution was washed with a saturated potassium fluoride solution (100 cm<sup>3</sup>) and water (100 cm<sup>3</sup>), dried (MgSO<sub>4</sub>) and then concentrated onto silica gel for purification by column chromatography (silica gel, dichloromethane/hexane 1/4). The compound was further purified by recrystallization from dichloromethane/ethanol to yield 3.80 g (79%) of the desired product. M.p. 123–125°C, purity >99% (GC). <sup>1</sup>H NMR (CDCl<sub>3</sub>) δ<sub>H</sub>: 7.21 (2H, dd), 7.48 (2H, d), 7.89 (2H, s), 8.12 (2H, d). MS (*m/z*): 300(M<sup>+</sup>).

**3.1.2. 4,7-bis(5-Bromothien-2-yl)-2,1,3-benzothiadiazole (3).** *N*-Bromosuccinimide (3.73 g, 0.0210 mol, freshly purified by recrystallization from water) was added slowly to a stirred solution of compound **2** (3.00 g, 0.0100 mol) in chloroform (100 cm<sup>3</sup>) and glacial acetic acid (100 cm<sup>3</sup>). The solution was heated under reflux for 1 h; dichloromethane (100 cm<sup>3</sup>) was added, and it was washed with water (100 cm<sup>3</sup>), hydrochloric acid (150 cm<sup>3</sup>, 20%), saturated aqueous sodium sulphite (50 cm<sup>3</sup>), and dried (MgSO<sub>4</sub>). The solvent was removed under reduced

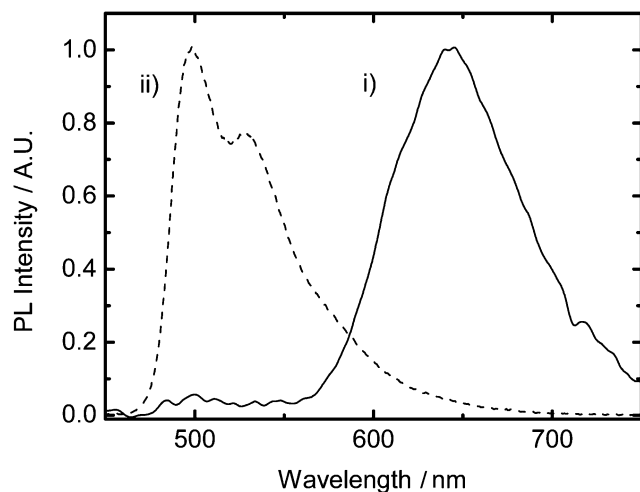


Figure 7. PL spectrum of (i) compound **9** doped in a green photopolymerized RM host **17** (full line), and of (ii) host **17** (dashed line) as a polymer network.

pressure and the product purified by recrystallization from toluene to yield 3.20 g (70%) of the desired product. M.p. 248–250°C, purity >99% (GC).  $^1\text{H NMR}$  ( $\text{CDCl}_3$ )  $\delta_{\text{H}}$ : 7.12 (2H, d), 7.77 (2H, s), 7.99 (2H, d). MS ( $m/z$ ): 460 ( $\text{M}^+$ ), 458 ( $\text{M}^+$ ), 456 ( $\text{M}^+$ ).

**3.1.3. 2-(4-Bromophenoxy)tetrahydropyran (5).** A mixture of 4-bromophenol (**4**) (20.0 g, 0.1156 mol), 3,4-dihydro-2H-pyran (10.6 g, 0.1262 mol) and *p*-toluenesulphonic acid monohydrate (0.01 g,  $5.26 \times 10^{-5}$  mol) was stirred in dichloromethane (150  $\text{cm}^3$ ) at ambient temperature for 1 h. The resultant solution was washed with water (200  $\text{cm}^3$ ), dried ( $\text{MgSO}_4$ ) and then concentrated onto silica gel for purification by column chromatography (silica gel, dichloromethane/hexane 1/1). The compound was further purified by recrystallization from ethanol to yield 22.1 g (74%) of the desired product. M.p. 58°C, purity >99% (GC).  $^1\text{H NMR}$  ( $\text{CDCl}_3$ )  $\delta_{\text{H}}$ : 1.56–1.73 (3H, m), 1.83–1.87 (2H, m), 1.93–2.04 (1H, m), 3.57–3.62 (1H, m), 3.83–3.89 (1H, m), 5.37 (1H, t), 6.93 (2H, d,  $J=9$  Hz), 7.36 (2H, d,  $J=9$  Hz). MS-EI ( $m/z$ ): 258 ( $\text{M}^+$ ), 256 ( $\text{M}^+$ ).

**3.1.4. 2-[4-(4,4,5,5-Tetramethyl-1,3,2)dioxaborolan-2-yl]-phenoxy]-tetrahydro-pyran (6).** *n*-Butyllithium in hexanes (18.7  $\text{cm}^3$ , 2.5M, 0.0467 mol) was added dropwise to a cooled ( $-78^\circ\text{C}$ ) solution of compound **5** (10.0 g, 0.0389 mol) in tetrahydrofuran (100  $\text{cm}^3$ ). The resultant solution was stirred at this temperature for 1 h and then 2-isopropoxy-4,4,5,5-tetramethyl-1,3,2-dioxaborolane (10.9 g, 0.0584 mol) was added dropwise while maintaining at  $-78^\circ\text{C}$ . Water (250  $\text{cm}^3$ ) was added and the resultant mixture extracted into diethyl ether ( $2 \times 200 \text{ cm}^3$ ). The combined organic layers were washed with water ( $2 \times 100 \text{ cm}^3$ ) and dried ( $\text{MgSO}_4$ ). After filtration the solvent was removed under reduced pressure to yield 6.7 g (56.5%) of the desired product. M.p. 28°C, purity >99% (GC).  $^1\text{H NMR}$  ( $\text{CDCl}_3$ )  $\delta_{\text{H}}$ : 1.33 (12H, s), 1.56–1.73 (3H, m), 1.84–1.88 (2H, m), 1.96–2.04 (1H, m), 3.57–3.61 (1H, m), 3.84–3.90 (1H, m), 5.48 (1H, t), 7.03 (2H, d,  $J=8.2$  Hz), 7.74 (2H, d,  $J=8.4$  Hz), MS-EI ( $m/z$ ): 304 ( $\text{M}^+$ ).

**3.1.5. 4,7-bis[2-(4-Hydroxyphenyl)thien-5-yl]-2,1,3-benzothiadiazole (8).** A mixture of tetrakis(triphenylphosphine)palladium(0) (0.13 g,  $1.10 \times 10^{-4}$  mol), compound **3** (1.00 g, 0.0022 mol), compound **6** (1.99 g, 0.0065 mol), tripotassium phosphate (0.0065 mol, 1.38 g) and DMF (40  $\text{cm}^3$ ) was heated at 80°C overnight. The cooled reaction mixture was extracted with dichloromethane ( $2 \times 80 \text{ cm}^3$ ) and the combined organic layers were washed with brine ( $2 \times 100 \text{ cm}^3$ ) and dried

( $\text{MgSO}_4$ ). After filtration the solvent was removed under reduced pressure and the residue purified by column chromatography on silica gel using dichloromethane as the eluant. The protected compound **7** was not characterized and the deprotection followed immediately. A mixture of **7** (0.72 g, 0.0011 mol) and *p*-toluenesulphonic acid monohydrate (1.00 g, 0.0053 mol) in dichloromethane/ethanol (1/1, 60  $\text{cm}^3$ ) was stirred at ambient temperature for 1 h. Water (250  $\text{cm}^3$ ) was added and the resultant mixture extracted into ethyl acetate ( $2 \times 50 \text{ cm}^3$ ). The combined organic layers were washed with brine ( $2 \times 50 \text{ cm}^3$ ) and dried ( $\text{MgSO}_4$ ). After filtration the solvent was removed under reduced pressure and the residue purified by column chromatography (silica gel, ethyl acetate/hexane 1/3) to yield 0.44 g (82%) of the desired product. M.p. >300°C (decomposition).  $^1\text{H NMR}$  ( $\text{CDCl}_3$ )  $\delta_{\text{H}}$ : 6.87 (4H, d,  $J=8.7$  Hz), 7.30 (2H, d,  $J=4$  Hz), 7.53 (4H, d,  $J=8.7$  Hz), 7.92 (2H, s), 8.12 (2H, d,  $J=4$  Hz), 9.38 (2H, s,  $-\text{OH}$ ), MS-EI ( $m/z$ ): 484 ( $\text{M}^+$ ).

**3.1.6. Red chromophore (9).** A mixture of **8** (0.44 g,  $9.09 \times 10^{-4}$  mol), 1,4-pentadien-3-yl 12-bromododecanoate (0.72 g,  $2.09 \times 10^{-3}$  mol) and potassium carbonate (0.38 g, 0.0027 mol) in DMF (40  $\text{cm}^3$ ) was heated at 90°C overnight. The cooled reaction mixture was filtered and the filtrate concentrated under reduced pressure. The crude product was purified by column chromatography (silica gel, ethyl acetate/hexane 1/5) followed by recrystallization from ethanol/dichloromethane to yield 0.42 g (50%) of the desired product. Transition temperatures Cr 146 SmC 185 I ( $^\circ\text{C}$ ),  $^1\text{H NMR}$  ( $\text{CDCl}_3$ )  $\delta_{\text{H}}$ : 1.27–1.40 (24H, m), 1.46 (4H, quint), 1.64 (4H, quint), 1.79 (4H, quint), 2.41 (4H, t), 4.00 (4H, t), 5.23 (4H, dt), 5.32 (4H, dt), 5.74 (2H, tt), 5.80–5.89 (4H, m), 6.99 (4H, d,  $J=8.5$  Hz), 7.25 (2H, d,  $J=4$  Hz), 7.58 (4H, d,  $J=8.5$  Hz), 7.90 (2H, s), 8.10 (2H, d,  $J=4$  Hz), MS-MALDI ( $m/z$ ): 1013 ( $\text{M}^+$ ). Elemental analysis: theory C 71.11, H 7.16, N 2.76, S 9.49; found C 71.30, H 7.25, N 2.60, S 9.30%.

## 3.2. Electrochemical measurements

The ionization potentials of the reactive mesogens were measured electrochemically by cyclic voltammetry using a computer-controlled scanning potentiostat (Solartron 1285). The electron affinity was estimated by subtraction of the optical bandedge, taken as the energy of the onset of absorption of the compound, from the IP. The electron affinities of **9** and **14** were also obtained electrochemically and the values obtained in both cases agreed within  $\pm 0.05$  eV with the values obtained optically.



### 3.3. Device fabrication and measurements

The time-of flight measurements were carried out with pulses of UV light from a nitrogen laser at 337 nm incident to a cell of thickness 3  $\mu\text{m}$  containing the smectic materials [15]. Thin films of the materials were prepared by spin coating from a 0.5–2.0 wt % solution in chloroform onto an appropriate substrate. The photopolymerizable films were usually polymerized in a nitrogen-filled chamber using UV light from a helium-cadmium laser at 325 nm with a constant intensity of 50  $\text{mW cm}^{-2}$ . Quartz substrates were used for the PL measurements. A multilayer OLED was fabricated on a glass substrate ( $12 \times 12 \times 1 \text{ mm}^3$ ) covered with an ITO transparent anode and a polystyrene sulphonate/polyethylene dioxythiophene (PSS/PEDOT) EL grade layer (thickness 45 nm) deposited by spin-coating. The PSS/PEDOT layer was baked at 165°C for 5 min in order to cure the layer and remove volatile components. **14** was deposited as a uniform thin film (100 nm) by spin-coating (2 krpm) from a dilute solution (0.5 wt %) in chloroform followed by baking at 60°C for 5 min and then several hours under hard vacuum to remove solvent. A crosslinked polymer network was formed by polymerizing the layer of **14** with light from a HeCd laser at 325 nm with a fluence of 500  $\text{J cm}^{-2}$ . The polymerization was carried out in the supercooled smectic phase at 60°C. A hole-blocking layer (6 nm) of commercially available (H. W. Sands) 3-(4-biphenyl)-4-phenyl-5-*tert*-butylphenyl-1,2,4-triazole (TAZ) was deposited on top of the crosslinked emission layer by vacuum deposition under a vacuum of  $10^{-6}$  mbar or better. Layers of lithium fluoride (1 nm) and then aluminium (80 nm) were deposited by vacuum deposition as a combined cathode. A uniformly aligned film of **14** was obtained by spinning onto a glass substrate coated with rubbed PEDOT. The substrate was heated to 68°C, quickly cooled to 60°C and then cooled at  $1^\circ\text{C min}^{-1}$  to room temperature to obtain uniform alignment. All the processing was carried out in a glove box filled with dry nitrogen (99.99% purity) to avoid oxygen and moisture contamination. PL was measured with the samples mounted in a chamber filled with dry nitrogen using a photodiode array (Ocean Optics S2000) with a spectral range of 200 to 850 nm and a resolution of 2 nm. EL was measured using a Labview controlled, Agilent E3631A d.c. power supply with a Minolta LS100 luminance meter and Avaspec 2048 fibre spectrometer.

### Acknowledgments

We express our thanks to the EPSRC for the award of a studentship to M. P. A. and S. P. K. We would also like

to thank B. Worthington ( $^1\text{H NMR}$ ) and K. Welham (MS) for spectroscopic measurements.

### References

- [1] C.D. Müller, A. Falcou, N. Reckefuss, M. Rojahn, V. Wiederhirm, P. Rudati, H. Frohne, O. Nuykens, H. Becker, K. Meerholz. *Nature*, **421**, 829 (2003).
- [2] A.E.A. Contoret, S.R. Farrar, P.O. Jackson, L. May, M. O'Neill, J.E. Nicholls, S.M. Kelly, G.J. Richards. *Adv. Mater.*, **12**, 971 (2000).
- [3] M. Jandke, D. Hanft, P. Strohrriegel, K. Whitehead, M. Grell, D.D.C. Bradley. *Proc. SPIE*, **4105**, 338 (2001).
- [4] P. Strohrriegel, D. Hanft, M. Jandke, T. Pfeuffer. *Mat. Res. Soc. Symp. Proc.*, **709**, 31 (2002).
- [5] S.M. Kelly, M. O'Neill. In *Handbook of Electroluminescence*, D.R. Vij (Ed.), p. 583, IOP (2004) and references therein.
- [6] M. O'Neill, S.M. Kelly. *Adv. Mater.*, **15**, 1135 (2004).
- [7] M. O'Neill, S.M. Kelly. *Ekisho.*, **9**, 9 (2005).
- [8] A.E.A. Contoret, M.P. Aldred, P. Vlachos, S.R. Farrar, W.C. Tsoi, M. O'Neill, S.M. Kelly. *Adv. Mater.*, **17**, 1368 (2005).
- [9] M.P. Aldred, P. Vlachos, A.E.A. Contoret, S.R. Farrar, W.C. Tsoi, B. Mansoor, K.L. Woon, R. Hudson, M. O'Neill, S.M. Kelly. *J. mater. Chem.*, **15**, 3208 (2005).
- [10] A. Bacher, P.G. Bentley, P. Glarvey, K.S. Whitehead, D.D.C. Bradley, M. Grell, M. Turner. *J. mater. Chem.*, **9**, 2985 (1999).
- [11] A. Bacher, P.G. Bentley, D.D.C. Bradley, L.K. Douglas, P. Glarvey, M. Grell, K.S. Whitehead, M. Turner. *Synth. Met.*, **111–112**, 413 (2000).
- [12] A.J. Eastwood, A.E.A. Contoret, S.R. Farrar, S. Fowler, S.M. Kelly, S.M. Khan, J.E. Nicholls, M. O'Neill. *Synth. Met.*, **121**, 1659 (2001).
- [13] A.E.A. Contoret, S.R. Farrar, P.O. Jackson, M. O'Neill, J.E. Nicholls, S.M. Kelly, G.J. Richards. *Synth. Met.*, **121**, 1645 (2001).
- [14] A.E.A. Contoret, S.R. Farrar, M. O'Neill, J.E. Nicholls, G.J. Richards, S.M. Kelly, A.W. Hall. *Chem. Mater.*, **14**, 1477 (2002).
- [15] M.P. Aldred, A.J. Eastwood, S.M. Kelly, P. Vlachos, B. Mansoor, M. O'Neill, W.-C. Tsoi. *Chem. Mater.*, **16**, 4928 (2004).
- [16] S. Méry, D. Haristoy, J.-F. Nicoud, D. Guillon, S. Diele, H. Monobe, Y. Shimizu. *J. mater. Chem.*, **12**, 37 (2002).
- [17] M. Funahashi, J.-I. Hanna. *Appl. Phys. Lett.*, **73**, 3733 (1998); *Mol. Cryst. liq. Cryst.*, **331**, 509 (1999); H. Maeda, M. Funahashi, J.-I. Hanna. *Mol. Cryst. liq. Cryst.*, **366**, 369 (2001).
- [18] M. Funahashi, J.-I. Hanna. *Mol. Cryst. liq. Cryst.*, **368**, 303 (2001).
- [19] K. Kogo, H. Maeda, H. Kato, M. Funahashi, J.-I. Hanna. *Appl. Phys. Lett.*, **75**, 3348 (1999).
- [20] P. Vlachos, S.M. Kelly, B. Mansoor, M. O'Neill. *Chem. Commun.*, 1874 (2002).
- [21] P. Vlachos, B. Mansoor, S.M. Kelly, M.P. Aldred, M. O'Neill. *Chem. Commun.*, 2921 (2005).
- [22] I. McCulloch, W. Zhang, M. Heeney, C. Bailey, M. Giles, D. Graham, M. Shkunov, D. Sparrowe, S. Tierney. *J. mater. Chem.*, **13**, 2436 (2003).
- [23] M. Millaruelo, L. Oriol, J.L. Serrano, M. Pinol, P.L. Sáez. *Mol. Cryst. liq. Cryst.*, **411**, 451 (2004).

- [24] J. Barche, S. Janietz, M. Ahles, R. Schmechel, H. Seggern. *Chem. Mater.*, **16**, 4286 (2004).
- [25] M.P. Aldred, P. Vlachos, D. Dong, S.P. Kitney, W.C. Tsoi, M. O'Neill, S.M. Kelly. *Liq. Cryst.*, **32**, 951 (2005).
- [26] K. Pilgram, M. Zupan, R. Skiles. *J. heterocycl. Chem.*, **7**, 629 (1970).
- [27] J.K. Stille. *Angew. Chem. int. Ed.*, **25**, 508 (1986).
- [28] M. Ranger, M. Leclerc. *Macromolecules*, **32**, 3306 (1999).
- [29] N. Miyaura, T. Yanagi, A. Suzuki. *Synth. Commun.*, **11**, 513 (1981).
- [30] R.D. Stephens, C.E. Castro. *J. org. Chem.*, **23**, 3313 (1963).
- [31] S.R. Farrar, A.E.A. Contoret, M. O'Neill, J.E. Nicholls, G.J. Richards, S.M. Kelly. *Phys. Rev. B*, **66**, 125107 (2002).
- [32] P. Dyreklev, M. Berggren, O. Inganas, M.R. Anderson, O. Wennerstrom, T. Hjertberg. *Adv. Mater.*, **7**, 43 (1995).
- [33] M. Grell, D.D.C. Bradley, E.P. Woo, M. Inbasekaran. *Adv. Mater.*, **10**, 9 (1997).
- [34] D. Neher. *Macromol. rapid Commun.*, **22**, 1366 (2001).
- [35] D. Sainova, A. Zen, H.G. Nothofer, U. Asawapirom, U. Scherf, R. Hagen, T. Bieringer, S. Kostromine, D. Neher. *Adv. func. Mater.*, **12**, 49 (2002).
- [36] S.W. Culligan, Y.H. Geng, S.H. Chen, K. Klubeck, K.M. Vaeth, C.W. Tang. *Adv. Mater.*, **15**, 1176 (2003).
- [37] Y.H. Geng, S.W. Culligan, A. Trajkovska, J.U. Wallace, S.H. Chen. *Chem. Mater.*, **15**, 542 (2003).
- [38] R. Güntner, T. Farrell, U. Scherf, T. Miteva, A. Yasuda, G. Nelles. *J. mater. Chem.*, **14**, 2622 (2004).
- [39] A.C.A. Chen, S.W. Culligan, Y.H. Geng, S.H. Chen, K. Klubeck, K.M. Vaeth, C.W. Tang. *Adv. Mater.*, **16**, 1176 (2004).
- [40] H. Tokuhisa, M. Era, T. Tsutsui. *Appl. Phys. Lett.*, **72**, 2639 (1998).
- [41] K. Kogo, T. Goda, M. Funahashi, J.-I. Hanna. *Appl. Phys. Lett.*, **73**, 1595 (1998).
- [42] M.P. Aldred, A.E.A. Contoret, P.E. Devine, S.R. Farrar, R. Hudson, S.M. Kelly, G.C. Koch, M. O'Neill, W.C. Tsoi, K.L. Woon, P. Vlachos. In *Organic Thin-Film Electronics*, A.C. Arias, N. Tessler, L. Burgi, J.A. Emerson (Eds), Materials Research Society Symposium Proceedings 871E, Warrendale, PA (2005).